Dynamic Neural Network-based System Identification of a Pressurized Water Reactor

Amine Naimi, Jiamei Deng, Altahhan Abdulrahman, Vineet Vajpayee, Victor Becerra, Nils Bausch

***Abstract*— This work presents a dynamic neural network-based (DNN) system identification approach for a pressurized water nuclear reactor. The presented empirical modelling approach describes the DNN structure using differential equations. Local optimization algorithms based on unconstrained Quasi-Newton and interior point approaches are used in the identification process. The efficacy of the proposed approach has been demonstrated by identifying a nuclear reactor core coupled with thermal-hydraulics. DNNs are employed to train the structure and validate it using the nuclear reactor data. The simulation results show that the neural network identified model is sufficiently able to capture the dynamics of the nuclear reactor and it is suitably able to approximate the complex nuclear reactor system.**

***Index Terms*— Dynamic Neural Network, System Identification, Modelling and Simulation, Pressurized Water Reactor.**

I. Introduction

A nuclear reactor is a complex non-linear system whose modelling using first-principles based approaches is a strenuous task due to parameter variations, internal reactivity feedbacks, parameter uncertainties, and unknown disturbances. System parameters associated with reactor core, thermal-hydraulics, and internal reactivity feedbacks differ significantly with operating power levels. On the other hand, the empirical modelling or system identification is a systematic way of constructing a mathematical model of a dynamical system from the measurement data.

In the last two decades, artificial neural networks (ANNs) have been applied to the modelling and control of nuclear reactors [1]–[7]. ANN possess good approximation abilities for non-linear systems [8]–[11]. Among the approaches used for NPP modelling and identification, the most applied architecture has been the recurrent multilayer perceptron [12]. The application of ANN-based techniques has shown effective results. ANN has been applied to design soft-computing-based control techniques. A diagonal recurrent neural network-based controller is proposed to enhance the temperature response of a PWR [4]. ANN-based controller using the response of a self-tuning regulator has been applied for wide-range power regulation [5]. An adaptive feed-forward ANN-based controller is proposed for the power level control of PWR [6]. The learning abilities of an ANN has been integrated with the decision-making capabilities of fuzzy logic to develop a neuro-fuzzy power controller [7].

Dynamic neural networks (DNNs) are outlined to be especially well suited for modelling non-linear systems [13]–[17]. DNN can address time-dependent behaviour to include transient phenomena and delay effects. These networks can approximate multi-variable non-linear dynamical systems and can be represented by non-linear state-space models. These properties make them suitable to be used together with nonlinear approaches such as feedback linearization technique. In this work, a special DNN structure is implemented for the identification of the PWR nuclear reactor. This DNN consists of only one single-layer network, which is favourable for control synthesis.

The rest of the paper is organized as follows: Section II introduces the model of the non-linear PWR system. Section III presents the identification strategy using DNNs. Section IV presents DNN identification using local optimisation techniques. Section V demonstrates the simulation results. Finally, conclusions are drawn in section VI.

II. Non-linear PWR Model

The core neutronics model can be expressed by the point kinetics equations coupled with delayed neutrons precursors' concentration [18] as,

$$\frac{dP}{dt} = \frac{\rho_t - \sum_{i=1}^{6} \beta_i}{\Lambda} P + \sum_{i=1}^{6} \lambda_i C_i, \tag{1}$$

$$\frac{dC_i}{dt} = \frac{\beta_i}{\Lambda} P - \lambda_i C_i, \qquad i = 1, 2, \ldots 6. \tag{2}$$

where P and C_i are neutronic power and delayed neutron precursors' concentration, respectively. λ_i and β_i are decay constant and fraction of delayed neutrons, respectively. Λ is prompt neutron life time and ρ_t is total reactivity.

The neutronic model is lumped with core thermal-hydraulics model to include reactivity feedback from fuel and coolant temperatures [19]. The core thermal-hydraulics model considered two lumps for representing coolant and one lump to denote the fuel node. The model is given by,

$$\frac{dT_f}{dt} = H_f P_n - \frac{1}{\tau_f}\left(T_f - T_{c1}\right), \tag{3}$$

$$\frac{dT_{c1}}{dt} = H_c P_n + \frac{1}{\tau_c}\left(T_f - T_{c1}\right) - \frac{2}{\tau_r}\left(T_{c1} - T_{cin}\right), \tag{4}$$

$$\frac{dT_{c2}}{dt} = H_c P_n + \frac{1}{\tau_c}\left(T_f - T_{c1}\right) - \frac{2}{\tau_r}\left(T_{c2} - T_{c1}\right). \tag{5}$$

Amine Naimi (amine.naimi01@gmail.com), Jiamei Deng (j.deng@leedsbeckett.ac.uk), and Altahhan Abdulrahman (a.altahhan@leedsbeckett.ac.uk) are with School of Built Environment, Engineering, and Computing, Leeds Beckett University, Leeds, LS6 3QS, United Kingdom.

Vineet Vajpayee (vineet.vajpayee@port.ac.uk), Victor Becerra (victor.becerra@port.ac.uk), and Nils Bausch (nils.bausch@port.ac.uk) are with School of Energy and Electronic Engineering, University of Portsmouth, Portsmouth, PO1 3DJ, United Kingdom.

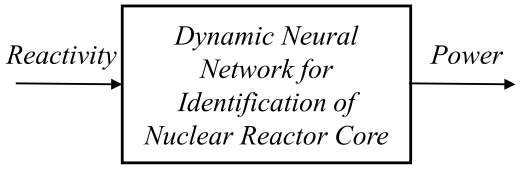

Fig. 1: Reactor core identification.

where T_f, T_{c1}, and T_{c2} denote the temperatures at fuel, coolant node 1 and node 2, respectively. H_f and H_c are proportionality constants. τ_f, τ_c, and τ_r are time constants. The effects of variation in temperatures of fuel and coolants are considered in terms of reactivity feedback. Thus, the total reactivity is given by

$$\begin{aligned} \rho_t &= \rho_{rod} + \rho_f + \rho_{c1} + \rho_{c2} \\ \rho_t &= \rho_{rod} + \alpha_f T_f + \alpha_c \left(T_{c1} + T_{c2}\right) \end{aligned} \tag{6}$$

where ρ_{rod}, ρ_f, ρ_{c1}, and ρ_{c2} denote the reactivity due to control rod, fuel temperature, coolant temperature at node 1 and 2, respectively. α_f and α_c denote the temperature coefficients of reactivity due to fuel and coolant, respectively.

III. System Identification Using DNN

A. Input Design

In this work, for the system identification of the nuclear reactor, the reactivity and neutronic power are used as input to and output from the system. The block diagram representation of the proposed architecture is given in Fig. 1. The input reactivity signal is chosen with random steps so as to exhibit the non-linear behaviour of the dynamic system. The input signal consists of a discrete time signal where random amplitude may occur at different sample time with a probability,

$$u\left(k\right) = \begin{cases} u\left(k-1\right), \text{with probability } \left(1-\alpha\right), \\ b + e\left(k\right), \text{with probability } \left(\alpha\right). \end{cases} \tag{7}$$

where $e\left(k\right)$ is a Gaussian random signal with the mean value b. The PWR model described by (1–6) is perturbed by the reactivity input. The estimation data is then formed with input as reactivity and power as output. The input signal is designed such that it is persistently excited to ensure that the data contain enough useful information. This will allow to obtain a good estimate of the model.

B. DNN Model Structure

DNNs have the characteristics of not only receiving external inputs but also allow neurons to have feedback connections with themselves, in other words they deal with the processing of the past knowledge and store the current information for the next stage. In this paper, a single layer of DNN is used to identify the dynamics. The DNN can be

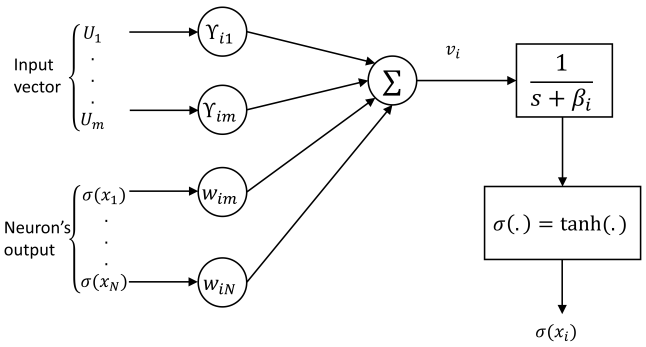

Fig. 2: A dynamic neuron.

expressed as follows:

$$\begin{aligned} \dot{x}(t) &= f\left(x\left(t\right), u\left(t\right), \theta\right) \\ \hat{y}(t) &= h\left(x\left(t\right), \theta\right) \end{aligned} \tag{8}$$

where $x \in \mathbb{R}^N$ are the states of the network, $u \in \mathbb{R}^m$, is the external input, θ is a vector of parameters of the network, and $y \in \mathbb{R}^p$ is the output. f and h are functions that represent the structure of the network and the relationships between the output and state, respectively.

It is known that the internal state of the output units of a continuous time DNN are capable to approximate any finite time trajectory of a given dynamic system [16]. The structure of the DNN used in this study is a specific case of (8) and an illustration of the DNN structure is given in Fig. 2 [14]. Here, the structure is defined by a one-dimensional array of N neurons and can be expressed as follows:

$$\dot{x}_i = -\beta_i x_i + \sum_{j=1}^{N} \omega_{ij} \sigma\left(x_j\right) + \sum_{j=1}^{m} \gamma_{ij} u_j \tag{9}$$

where β_i, ω_i, and γ_i are adjustable weights. The vectored form of (9) is given by:

$$\dot{x} = -\beta x + \omega \sigma\left(x\right) + \gamma u \tag{10}$$

$$\hat{y} = Cx \tag{11}$$

where x are coordinates on $\mathbb{R}^N$, $\omega \in \mathbb{R}^{N \times N}$, $\sigma\left(x\right) = \left[\sigma\left(x_1\right) \cdots \sigma\left(x_N\right)\right]^T$, $\gamma \in \mathbb{R}^{N \times m}$, $u \in \mathbb{R}^m$, $C = \left[I_{p \times p}\ 0_{p \times (N-p)}\right]$, and $\beta \in \mathbb{R}^{N \times N}$ is a diagnosable matrix with diagonal elements $\left\{\beta_1 \cdots \beta_N\right\}$.

IV. Optimisation-based DNN Identification

The block diagram of the proposed identification scheme is shown in Fig. 3. The algorithm tunes the parameters of the DNN identified model to match the response of the identified model with the measurement data of the real plant. This is done by minimizing the quadratic objective function formed using the measured and estimated outputs. The nonlinear unconstrained optimization problem [14] can be formulated

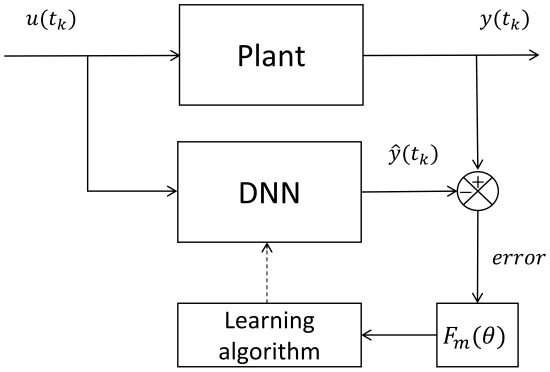

Fig. 3: Optimisation-based DNN identification scheme.

as,

$$\min_{\theta} F_m(\theta, Z_m) = \frac{1}{2M}\sum_{k=1}^{M} \|y(t_k) - \hat{y}(t_k|\theta)\|^2 \quad (12)$$

where $Z_m = \left[y(t_k)\ u(t_k)\right]_{k=1,2\cdots,M}$ is a training dataset, θ is a parameter vector, $y(t_k)$ is the measured output, and $\hat{y}(t_k|\theta)$ is the estimated output. Eq. (12) can be solved using local optimization techniques which estimate the optimal value within a neighbouring set of candidate solutions. A wide spectrum of methods exists for local optimization [20]. Among them, two gradient-based approaches, Quasi-Newton and Interior-Point algorithms are employed here.

A. Quasi-Newton Algorithm

Quasi-Newton methods have been developed for solving nonlinear equations that result from a minimization problem. The principle of these iterative algorithms is to progress step by step from an initial point θ_0 along line search directions h_k in order to converge on the desired optimal point θ_{opt}. At the kth stage of the algorithm, the inverse of the hessian matrix H_k is computed to find the search direction. The basic form of the algorithm is described by the following steps:

1) Choose an initial point θ_0 and initialize H_0 (usually $H_0 = I$)
2) Compute the gradient $\nabla f(\theta_k)$ and the direction search $h_k = -H_k \nabla f(\theta_k)$
3) Perform a line search from θ_k in the direction h_k using the following equation: $\theta_{k+1} = \theta_k + T_s h_k$, where T_s is the step size
4) Compute H_{k+1} and go back to step 2.

The Quasi-Newton algorithm employed here is the Broyden-Fletcher-Goldfarb-Shanno algorithm [21] and can be defined as follows:

$$H_{k+1} = H_k + \frac{q_k q_k^T}{q_k^T s_k} - \frac{H_k s_k s_k^T H_k^T}{s_k^T H_k s_k} \quad (13)$$

where $s_k = \theta_{k+1} - \theta_k$ is the parameter change between two iterations and $q_k = \nabla f(\theta_{k+1}) - \nabla f(\theta_k)$ is the gradient change between two iterations.

B. Interior-Point Algorithm

Interior-Point methods solve linear as well as nonlinear convex optimization problems that contain inequalities as constraints [22]. The optimisation problem minimizes the objective function subjected to sub-nonlinear equality constraints ($h(\theta) = 0$) and variable inequality constraints ($g(\theta) \leq 0$). It can be written as follows:

$$\min_{\theta} F_m(\theta),\ \text{subject to } h(\theta) = 0 \text{ and } g(\theta) \leq 0 \quad (14)$$

Interior-point methods also referred as barrier methods. The deviation of these methods associates with (12) the barrier problem:

$$\min_{\theta,s} F_m(\theta) = \min F_m(\theta) - \mu \sum_i \log(s_i),$$
$$\text{subject to } h(\theta) = 0 \text{ and } g(\theta) + s = 0 \quad (15)$$

where μ is a positive parameter, s_i are the slack variables and log is the logarithm function. The barrier approach consists of finding solutions of the barrier problem for a sequence of positive barrier parameters μ_k that converges to zero.

V. Simulation Results

The technique presented in the previous section has been applied to identify the PWR model. A case study is carried out to train and validate the identified DNN-based identified PWR model by applying the input signal with random steps. The training of the DNN is carried out using the Quasi-Newton and Interior-Point algorithms. The best model is found to be of second-order. The DNN model structure can be represented as follows:

$$\dot{x}_1 = -\beta_1 x_1 + \omega_{11}\sigma(x_1) + \omega_{12}\sigma(x_2) + \gamma_1 u \quad (16)$$
$$\dot{x}_2 = -\beta_2 x_2 + \omega_{21}\sigma(x_1) + \omega_{22}\sigma(x_2) + \gamma_2 u \quad (17)$$
$$y = Cx \quad (18)$$

The parameters of the Quasi-Newton (Q-N) estimated DNN model is as follows:

$$\beta = \begin{bmatrix} 0.5767 & 0 \\ 0 & -0.1038 \end{bmatrix}; \omega = \begin{bmatrix} -0.4523 & 0.7762 \\ -0.1850 & -0.3670 \end{bmatrix};$$
$$\gamma = \begin{bmatrix} 0.620\ 0.1837 \end{bmatrix}^T; C = \begin{bmatrix} 1\ 0 \end{bmatrix}. \quad (19)$$

The parameters of the Interior-Point (I-P) estimated DNN model is as follows:

$$\beta = \begin{bmatrix} 1.161 & 0 \\ 0 & -0.0326 \end{bmatrix}; \omega = \begin{bmatrix} -1.8181 & 1.0324 \\ -0.1320 & -0.0945 \end{bmatrix};$$
$$\gamma = \begin{bmatrix} 1.3223\ -0.0361 \end{bmatrix}^T; C = \begin{bmatrix} 1\ 0 \end{bmatrix}. \quad (20)$$

Fig. 4 shows the designed training input and the corresponding output employed for the model estimation exercise. Fig. 4b plots the output of the models estimated by the Quasi-Newton and Interior-Point algorithms for the reactivity input shown in Fig. 4a. It compares the measures output with the estimated model responses. Both the algorithms are sufficiently able to estimate the non-linear behaviour.

Fig. 5 shows the validation dataset employed for model validation. The validation data is selected such that it is

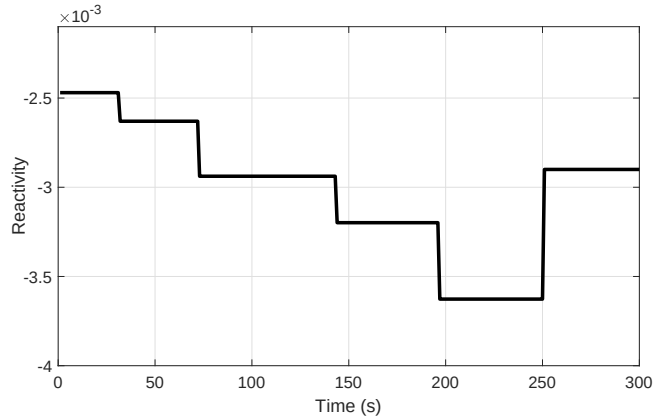

(a) Training input trajectory.

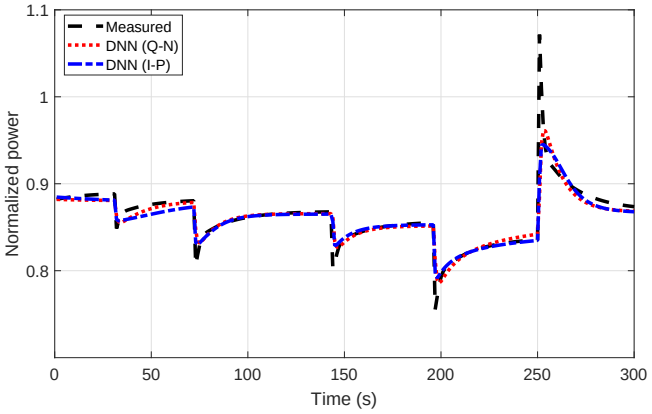

(b) Training output trajectory.

Fig. 4: Variation of measured and estimated normalized power signals Quasi-Newton and Interior-Point algorithms.

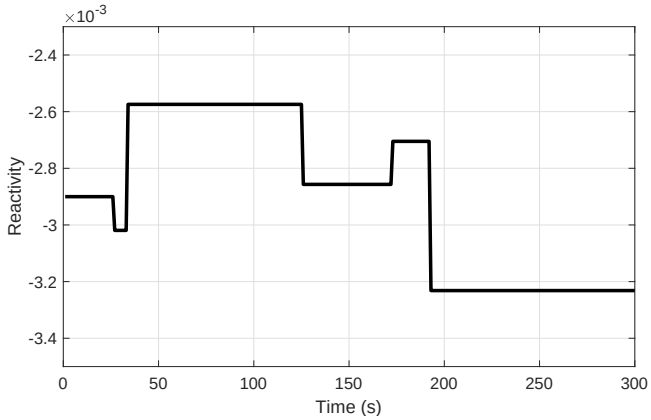

(a) Validation input trajectory.

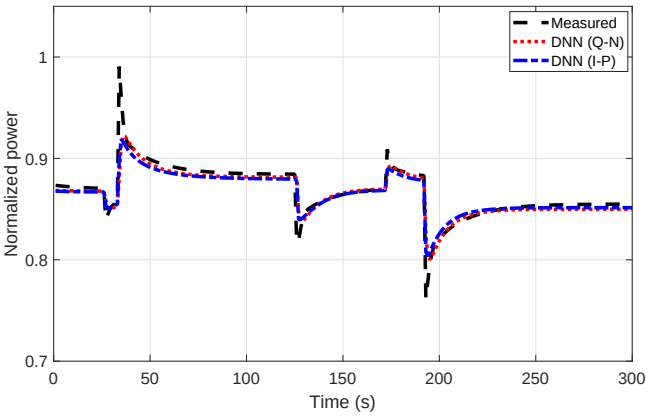

(b) Validation output trajectory.

Fig. 5: Variation of measured and estimated normalized power signals Quasi-Newton and Interior-Point algorithms.

different from the estimation data so as to test the capabilities of the identified models. The validation input is plotted in Fig. 5a and the corresponding model response is plotted in Fig. 5b. Both the estimated models can track the measured response. Another validation dataset is chosen to validate the performance of the estimated models. Fig. 6 shows the validation dataset employed for model validation. The validation input is plotted in Fig. 6a and the corresponding model response is plotted in Fig. 6b. It can be observed that both the DNN identified models are sufficiently able to track the measured power signal over a large range. The good estimation and validation outcomes in both cases are due to the good non-linear approximation capabilities of the DNN identified model, however, it can be noticed that the two DNNs are not tracking well the system output when this is presenting peaks. The proposed non-linear approach is able to approximate the reactor process with a second-order DNN identified model thereby reducing the model order significantly.

A quantitative performance assessment is conducted by computing the root mean squared error (RMSE) between the measured output and the estimated response. It is given by,

$$RMSE = \sqrt{\frac{1}{K}\sum_{i=1}^{K}(y_i - \hat{y}_i)^2}, \tag{21}$$

where K is the total number of samples. y_i and $\hat{y}_i$ are measured output and estimated output, respectively. Table I compares the modelling performances of the Quasi-Newton and Interior-Point algorithms. It is found that the values of RMSE for both the approaches are similar. Both the local optimization technique perform equally well, however, the Quasi-Newton algorithm gives slightly better performance over the Interior-Point algorithm. These simulation results show acceptable performance of the obtained DNN model. For further performance improvement, global optimization algorithms such as direct and genetic algorithms can be used as part of the DNN training. This will further reduce the estimation error and thus will improve the modelling performance.

VI. Conclusions

In this study, a system identification technique based on a single layer DNN structure is presented for the identification

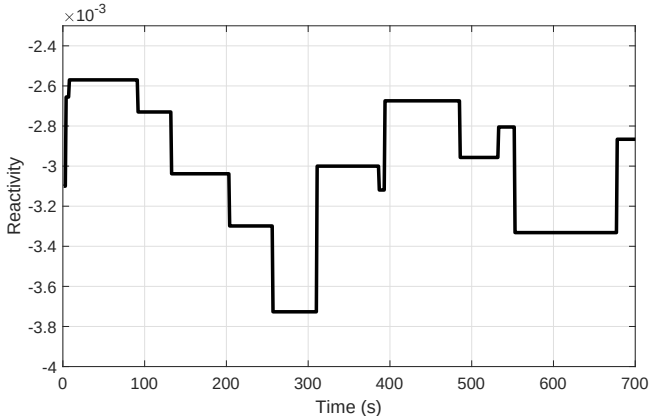

(a) Validation input trajectory.

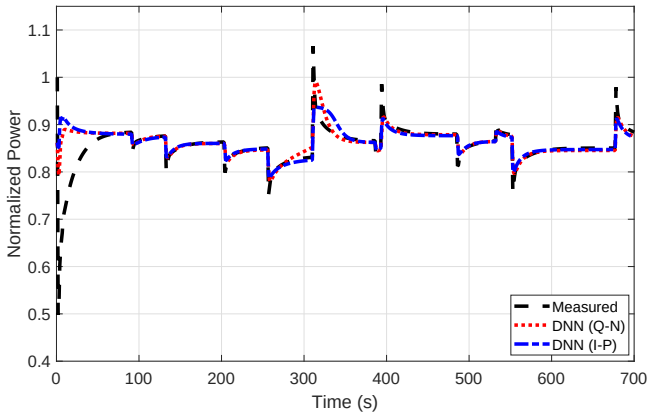

(b) Validation output trajectory.

Fig. 6: Variation of measured and estimated normalized power signals Quasi-Newton and Interior-Point algorithms.

TABLE I: Root mean squared error

Model	Training	Validation-I	Validation-II
Q-N	1.87×10^{-4}	1.56×10^{-4}	3.41×10^{-2}
I-P	9.50×10^{-5}	7.99×10^{-5}	3.87×10^{-2}

of a PWR-type nuclear reactor. Unconstrained Quasi-Newton and Interior-Point algorithms are used for the identification process. The results demonstrate that the obtained DNN can achieve accurate estimation performance. The proposed DNN has the advantage of simple structures, which makes it convenient to be used for control design and especially to be applied together with feedback linearisation approach. The future work will be to design a control strategy based on the proposed DNN model.

VII. Acknowledgement

The work presented in this paper has been financially supported under grants EP/R021961/1, EP/R022062/1, and EP/M018717/1 from the Engineering and Physical Sciences Research Council.

References

[1] M. Boroushaki, M. B. Ghofrani, C. Lucas, and M. J. Yazdanpanah, "Identification and control of a nuclear reactor core (vver) using recurrent neural networks and fuzzy systems," *IEEE Transactions on Nuclear Science*, vol. 50, no. 1, pp. 159–174, 2003.

[2] Z. Gang, C. Xin, Y. Weicheng, and P. Wei, "Identification of dynamics for nuclear steam generator water level process using rbf neural networks," in *2007 8th International Conference on Electronic Measurement and Instruments*, 2007, pp. 3379–3383.

[3] T. Adali, B. Bakal, M. Sonmez, R. Fakory, and C. Tsaoi, "Modeling nuclear reactor core dynamics with recurrent neural networks," *Neurocomputing*, vol. 15, no. 3, pp. 363 – 381, 1997.

[4] C. C. Ku, K. Y. Lee, and R. M. Edwards, "Improved nuclear reactor temperature control using diagonal recurrent neural networks," *IEEE Transactions on Nuclear Science*, vol. 39, no. 6, pp. 2298–2308, 1992.

[5] M. N. Khajavi, M. B. Menhaj, and A. A. Suratgar, "A neural network controller for load following operation of nuclear reactors," *Annals of Nuclear Energy*, vol. 29, no. 6, pp. 751 – 760, 2002.

[6] H. Arab-Alibeik and S. Setayeshi, "Adaptive control of a pwr core power using neural networks," *Annals of Nuclear Energy*, vol. 32, no. 6, pp. 588 – 605, 2005.

[7] S. S. Khorramabadi, M. Boroushaki, and C. Lucas, "Emotional learning based intelligent controller for a pwr nuclear reactor core during load following operation," *Annals of Nuclear Energy*, vol. 35, no. 11, pp. 2051 – 2058, 2008.

[8] S. CHEN, S. A. BILLINGS, and P. M. GRANT, "Non-linear system identification using neural networks," *International Journal of Control*, vol. 51, no. 6, pp. 1191–1214, 1990.

[9] K. S. Narendra and K. Parthasarathy, "Identification and control of dynamical systems using neural networks," *IEEE Transactions on Neural Networks*, vol. 1, no. 1, pp. 4–27, 1990.

[10] Chi-Hsu Wang, Pin-Cheng Chen, Ping-Zong Lin, and Tsu-Tian Lee, "A dynamic neural network model for nonlinear system identification," in *2009 IEEE International Conference on Information Reuse Integration*, 2009, pp. 440–441.

[11] Z. Aslipour and A. Yazdizadeh, "Identification of nonlinear systems using adaptive variable-order fractional neural networks (case study: A wind turbine with practical results)," *Engineering Applications of Artificial Intelligence*, vol. 85, pp. 462 – 473, 2019.

[12] A. G. Parlos, K. T. Chong, and A. F. Atiya, "Application of the recurrent multilayer perceptron in modeling complex process dynamics," *IEEE Transactions on Neural Networks*, vol. 5, no. 2, pp. 255–266, 1994.

[13] J. O. Pedro, M. Dangor, O. A. Dahunsi, and M. M. Ali, "Dynamic neural network-based feedback linearization control of full-car suspensions using pso," *Applied Soft Computing*, vol. 70, pp. 723 – 736, 2018.

[14] J. Deng, V. M. Becerra, and R. Stobart, "Predictive control using feedback linearization based on dynamic neural models," in *2007 IEEE International Conference on Systems, Man and Cybernetics*, 2007, pp. 2716–2721.

[15] V. M. Becerra, J. Deng, and S. Nasuto, "A novel dynamic neural network structure for nonlinear system identification," *IFAC Proceedings Volumes*, vol. 38, no. 1, pp. 348 – 353, 2005, 16th IFAC World Congress.

[16] F. Garces, V. Becerra, C. Kambhampati, and K. Warwick, *Strategies for feedback linearisation:a dynamic neural network approach*, 2002.

[17] J. Deng, "Dynamic neural networks with hybrid structures for nonlinear system identification," *Engineering Applications of Artificial Intelligence*, vol. 26, no. 1, pp. 281 – 292, 2013.

[18] V. Vajpayee, S. Mukhopadhyay, and A. P. Tiwari, "Multiscale subspace identification of nuclear reactor using wavelet basis function," *Annals of Nuclear Energy*, vol. 111, pp. 280 – 292, 2018.

[19] S. E. Arda and K. E. Holbert, "A dynamic model of a passively cooled small modular reactor for controller design purposes," *Nuclear Engineering and Design*, vol. 289, pp. 218 – 230, 2015.

[20] G. Venter, "Review of optimization techniques," *Encyclopedia of aerospace engineering*, 2010.

[21] J. E. Dennis Jr and R. B. Schnabel, *Numerical methods for unconstrained optimization and nonlinear equations*. SIAM, 1996.

[22] J. Nocedal and S. Wright, *Numerical optimization*. Springer Science & Business Media, 2006.